A TRANSMISSION ELECTRON MICROSCOPE INVESTIGATION OF SPACE WEATHERING EFFECTS IN HAYABUSA SAMPLES. Lindsay P. Keller[1] and Eve L. Berger[1,2]. [1]Robert M. Walker Laboratory for Space Science, ARES, Mail Code KR, NASA/JSC, Houston, TX 77058, [2]GeoControl Systems, Inc. – Jacobs JETS contract, NASA JSC, Houston, TX 77058. (Lindsay.P.Keller@nasa.gov).

Introduction. The Hayabusa mission to asteroid 25143 Itokawa successfully returned the first direct samples of the regolith from the surface of an asteroid. The Hayabusa samples thus present a special opportunity to directly investigate the evolution of asteroidal surfaces, from the development of the regolith to the study of the more complex effects of space weathering. Here we describe the mineralogy, microstructure and composition of three Hayabusa mission particles using transmission electron microscope (TEM) techniques.

Preliminary analyses of the Hayabusa samples show that their mineralogy and composition are consistent with an LL5-LL6 ordinary chondrite parent body with some less equilibrated LL4 petrographic-type material [1]. Abe et al. [2] presented near-infrared spectral data for Itokawa showing surface variations of up to 10% in absorption band depths and albedo that result from differences in space weathering effects and physical properties (e.g. grain size). Noguchi et al. [3] showed TEM data from several Hayabusa grains (olivine and pyroxene) with complex multi-layered rims and proposed that the rims formed through interaction with the solar wind. Many of the particle surfaces are decorated with $npFe^0$ as well as nanophase Fe-S grains (presumably troilite) [3].

Samples and Methods. We were allocated particles RA-QD02-0125 and RA-QD02-0211 from the JAXA collection, and RA-QD02-0192 from the NASA collection. The particles were embedded in low viscosity epoxy and thin sections were prepared using ultramicrotomy. High resolution images and electron diffraction data were obtained using a JEOL 2500SE 200 kV field-emission scanning-transmission electron microscope. Quantitative chemical maps and analyses were obtained using a Thermo-Noran thin-window energy-dispersive x-ray (EDX) spectrometer.

Results and Discussion. Particle RA-QD02-0125 is an ~37 μm olivine single crystal that contains μm-sized inclusions of FeS and is surrounded by a microstructurally complex rim that shows a mottled contrast in TEM images. The particle is rounded in shape and has numerous sub-μm grains attached to its surface including pyrrhotite, albite, olivine, augite, orthopyroxene and rare melt droplets. The composition of the olivine by TEM-EDX analyses is $Mg_{1.4}Fe_{0.6}SiO_4$ (Fo_{70}) and is homogeneous Solar flare tracks have not been observed within the olivine, and only an upper limit ($<10^9$ cm^{-2}) can be placed on the track density given the limitation imposed by the size of the fragments in the microtome thin sections. The particle is surrounded by a continuous ~50 nm thick, structurally disordered rim that is nanocrystalline with minor amorphous material between crystalline domains. We have not observed nanophase Fe metal grains within the disordered rim. Compositional profiles obtained from the core of the grain through the rim show no major chemical differences except for the outermost 5 nm which shows a slight Si-enrichment. The adhering melt droplets are dominated by Fe-sulfides although a few melt droplets are immiscible mixtures of silicate glass (~chondritic) with Fe metal/Fe sulfide blebs.

One of the surface adhering grains is a pyrrhotite grain that exhibits a strained rim on its exposed surface. EDX mapping of the strained/disordered rim shows that the outer ~8-10 nm thick zone is S-depleted with nanophase Fe metal grains (<5 nm) decorating the outermost surface. The microstructure of the S-depleted layer on the pyrrhotite grain in RA-QD02-0125 is similar to that observed in troilite irradiated with 4 kV He^+ ions to a fluence of ~10^{18} ions/cm^2 [4, 5]. The pyrrhotite also displays a complex superstructure in its core that is absent in the S-depleted rim. Prolonged irradiation has been shown to disorder pyrrhotite such that the superstructure reflections are lost [6].

Particle RA-QD02-0211 is an angular, ~41 μm olivine single crystal that contains μm-sized inclusions of FeS, solar flare particle tracks (Fig. 1), and also shows a structurally disordered rim ~100 nm thick. The solar flare track density is ~$2x10^{10}$ cm^{-2}. The disordered rim is nanocrystalline with minor amorphous material between crystalline domains. Quantitative element maps show the outermost ~10 nm of the disordered rim is Si-rich with lower Mg/Si and Fe/Si than the core of the grain and likely represents vapor or sputter deposited material. We observed regions within the rim that contain nanophase (2-5 nm) Fe metal particles in high resolution TEM images (Figure 2), but they are not uniformly distributed throughout the rim.

Particle RA-QD02-0192 is a polymineralic, rounded particle ~43 μm in size whose mineralogy is dominated by olivine (Fo_{70}) and lesser Ca-rich and Ca-poor pyroxene. Adhering grains include olivine, opx, albite, troilite and a sub-μm melt spherule. The olivine, orthopyroxene and augite in the core of the particle have damaged rims ~70 nm thick, similar to those seen in the other two particles. In addition, many of

the adhering grains also are surrounded by damaged rims. Solar flare tracks are present in olivine and albite, but the density is low ~$1x10^9$ cm^{-2}.

Rim Formation. The core and rim compositions on all three particles are very similar, consistent with an origin by solar wind radiation damage, as opposed to vapor or sputter deposition [7]. The Si-enrichment observed in the outermost few nanometers of the rims in -0211 and -0125 represents either the addition of vapor-/sputter-deposited material, or a thin zone of preferential sputtering. The structurally disordered rims on the Hayabusa particles likely result from atomic displacement damage from solar wind ions ions given the similarity of the rim thickness compared to the implantation depth of solar wind ions.

Surface Exposure. Solar flare energetic particles have a penetration depth of mm to cm and leave a trail of ionization damage in insulating materials. The solar flare track density correlates with exposure age as long as the grain was within a few cm of the parent body surface. From analyses of lunar rock samples, the solar flare track production rate at 1 AU is ~$6x10^5$ y^{-1} for a 2π exposure [8]. Asteroid Itokawa has a semi-major axis of 1.324 AU and so we use the Blanford et al. [8] rate for the Hayabusa samples. Based on this track production rate, and assuming that the particles had a single stage exposure in the Itokawa regolith, then the track density in particle RA-QD02-0211 corresponds to a minimum surface exposure of ~$3x10^4$ y. For particle RA-QD02-0192 the exposure is ~$2x10^3$ y, while we can only place an upper limit constraint on RA-QD02-0125 of <10^3 years, given its lack of observable tracks. Low track densities are difficult to measure in microtome thin sections owing to the chatter and disruption that results from the cutting process. We are developing a focused ion beam approach to preparing thin sections of Hayabusa particles that will enable more accurate measurement of track densities in the ~10^8 – 10^9 cm^{-2} range [9].

Conclusions. The three Hayabusa particles described here record the effects of space weathering processes on Itokawa. All three particles show microstructurally disordered rims that are still largely crystalline. Noguchi et al. [3] proposed that the disordered rims they observed on Itokawa particles largely result from solar wind radiation damage and we arrive at a similar conclusion for the particles we analyzed. We observed solar flare tracks in 2 of the 3 particles and the track densities are consistent with short surface exposures. The Hayabusa grains appear to lack the abundant melt spherules and vapor deposits that are common in lunar soil grains with a similar exposure history.

References. [1] Nakamura, T. *et al.* (2011) *LPSC XLII*, #1766. [2] Abe, M. *et al.* (2006) *Science* 312, 1334. [3] Noguchi, T. et al. (2013) *MAPS*, in press. [4] Loeffler, M. J. *et al.* (2008) *Icarus* 195, 622. [5] Keller, L. P. *et al.* (2010) *LPSC XLI*, #1172. [6] Christoffersen, R. and Keller, L. P. (2011) *MAPS* 46, 950. [7] Keller, L. P. and McKay, D. S. (1997) *GCA*, 61, 2331. [8] Blanford, G. E. *et al.* (1975) *PLPSC*, 6, 3557. [9] Berger, E. L. and Keller, L. P. (2014) this volume.

Acknowledgements. This work was supported by a NASA LARS Program grant to LPK.

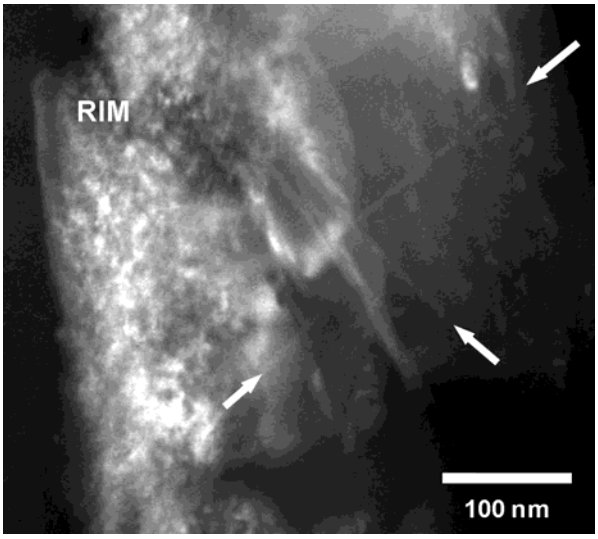

Figure 1. Dark-field STEM image of the disordered rim on the olivine in RA-QD02-0211. The arrows indicate solar flare tracks.

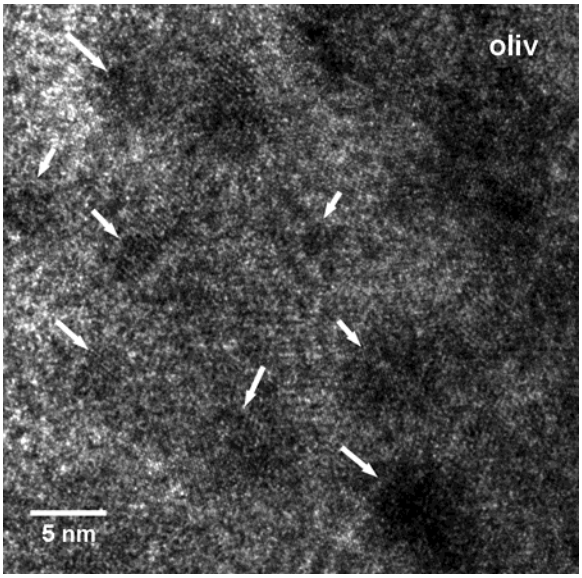

Figure 2. High resolution TEM image of the disordered rim on the olivine in RA-QD02-0211. The arrows indicate individual 2-5 nm $npFe^0$ particles in the crystalline olivine.